COMPRESSIVE LOADING TEST OF CORRODED GUSSET PLATE CONNECTION IN STEEL TRUSS BRIDGE

Jun Murakoshi[1], Naoki Toyama[1], Mamoru Sawada[1], Kentaro Arimura[1], Lu Guo[1]
Kuniei Nogami[2], Teruhiko Yoda[3], Hideyuki Kasano[3]

Abstract

With the stock aging of the majority of highway bridges in Japan constructed during the 1950s–1970s, some serious corrosion deterioration cases of fracture critical members in steel truss bridges have been reported recently. In this paper, compressive loading test of severely-corroded gusset plate connections cut out from a demolished truss bridge were conducted in order to assess the remaining load capacity.

Introduction

The majority of highway bridges in Japan were constructed during the 1950s–1970s which coincides with Japan's high economic growth period, and the number of bridges over 50 years is increasing drastically. With increase of aged bridges, since these bridges are exposed to heavy traffic and severe natural environment, it is highly probable that the deterioration and damage will increase rapidly. Improvement of technologies related to inspection, diagnosis, repair, and rehabilitation needed. Concerning steel bridges, some serious deterioration cases of FCMs on steel truss bridges have been reported recently. A tension diagonal member of steel truss embedded inside the deck concrete fractured in the Kiso River Bridge and Honjo Bridge on the National Route because of corrosion that invisibly progressed inside the concrete in 2007. Fracture of diagonal members or gusset plate connections of truss bridge is likely to lead to fatal damage of whole bridge. On the other hands, there was no effective measure to evaluate remaining strength of such deteriorated components and the whole bridge system with the uncertain section loss from corrosion.

The authors initiated research project in order to identify the remaining load capacity and to investigate how to evaluate the remaining strength of deteriorated diagonal members and riveted gusset plate connections subjected to severe corrosion. In this research project, several corroded specimens are going to be tested within a few years. These specimens consist of diagonals and gusset plate connections which were cut out from demolished steel bridges which were in service about 50 years near coastal area.

This paper reports the preliminary results from of compressive loading test of the first one specimen conducted in September, 2011, and discusses compressive behavior and the ultimate strength for severely-corroded gusset plate connection.

[1] Center for Advanced Engineering Structural Assessment and Research(CAESAR), Public Works Research Institute(PWRI)
[2] Department of Civil and Environmental Engineering, Tokyo Metropolitan University
[3] Department of Civil and Environmental Engineering, Waseda University

Before the test, section loss was measured using laser measurement equipment, and the effect of the section loss on failure behavior and the ultimate strength were examined by Finite Element analyses to complement experimental results. Then the authors compare experimental results with analysis results and strength equations in gusset plate connections.

Bridge Description

Figure 1 shows a bridge utilized in this project, which is called Choshi Bridge. It was built in 1962 across Tone River, called Choshi Bridge. It was 5-span steel through truss bridge with total length of 407.4m. Figure 2 shows general and section view of the bridge. The average daily traffic is about 20,000 with 10% of heavy vehicles. It was located in river mouth and had suffered from salt damage by airborne salt and heavily corroded. Although repainting, strengthening and partial replacement of severely corroded members were conducted several times through its service life, it was finally replaced in 2009 at 47 years old, because the corrosion was unlikely to stop and it is considered to be impossible to assess remaining strength and remaining service life.

Figure 3 shows corrosion damage focusing on main members and gusset plate connection that influence safety of the whole bridge. Steel members of this bridge have been repainted by the thick fluorine coating material, so section loss was not able to be observed exactly by visual inspection. Corrosion of gusset plate connections are shown in Figure 3(a) (b). Several connections and diagonals were strengthened with steel plate bonding (see Figure 3(c)). Intense corrosion of diagonal joint is shown in Figure 3(d). Pitting of diagonal was observed in Figure 3(e). Concerning floor beams, Figure 3 (f) shows typical area of deterioration of floor beam with debris accumulation.

Compression Load Test

Specimen Description and Experimental Setup

After demolished, several connection parts and diagonal members were cut out as experimental specimens, and carried to our laboratory after the coating was removed. For the present, we are planning to conduct the loading test for 4 specimens which have different gusset configurations. Figure 4 shows the first one test specimen, which was cut out from upper chord connection P25d near intermediate support. The diagonal is square box type section with flange of 500mm width and 10 and 12 mm thickness at the connection, and thickness of gusset plate is 12mm. Design axial force/stress of the diagonal members are listed in Table 1. Steel grade is SM40 (400MPa nominal tensile strength), the yield strength is 284MPa by tensile material test of the diagonal member.

Section loss at the outer and inner surface of the specimen was measured using laser surface measurement equipment (see Figure 5). The measurement interval was set to 1mm to understand the mechanical behavior for uneven surface. As it was difficult to measure the inner surface directly, the surface shape was taken using plaster, and then it was measured. Figure 6 shows contours of corrosion areas. Red area means large section loss, and yellow color means non-corrosion areas. Severe section loss was observed at connection parts of diagonal and gusset plate. As for the gusset plates, severe sections loss on the outer surface was not be seen except the rivets areas. Severe section was observed on the inner surface, where humidity seems high and airborne salt is likely to accumulate. As for the compression diagonal, large section loss on the outer surface was hardly found except the edge of flange, however, large section loss was shown on the inner surface around the gusset plate boundary. The maximum corrosion depth on the inner surface of the compression diagonal is 8.0mm (thickness of the diagonal flange: 12mm), the average corrosion depth is 3.4mm. The maximum and the average corrosion depths on the inner surface of the gusset plate are 9.0mm and 4.0mm respectively. The average corrosion depth at the plate area underneath the diagonal is 6.7mm. The average remaining thickness of the gusset plate is 8.0mm. The average reduction area ratio is 19% for the compression diagonal and 33% for the gusset plate. Comparing the measured section loss distribution with FE analysis results, it was found that severe corrosion part generally corresponded to the part where large stress appears. As a result, gusset plate connections may be structural weakpoint.

Figure 7 shows outline of specimen and loading frame. Figure 8 shows experimental setup. The compression and the tension axial loads were applied to the diagonal members at the same load increment step, because the absolute values of the design axial forces of both diagonals are almost equal. However, by the restrictioin of capacity of tension jack, tensile load was fixed to 2000kN. 30MN testing machine for compression and loading frame with jacks for tension were used for bi-axial loading.

Analysis Method

FE analyses were carried out to investigate the effect of section loss on compressive behavior by using a model shown in Figure 9. The analysis model simulated test condition. In modeling, 4 nodes shell elements were used for gusset plates and diagonals. Rivet fasteners were modeled by spring elements. The stress-strain relation of steel was assumed to be bi-linear, with a second modulus of $E/100(E=2\times10^5$MPa). Upper chord was restrained with the loading frame at connection part. The displacement along the loading direction at the loading point is free, and the displacements of two other directions are fixed. In this analysis, the initial imperfection is not considered.

Analyses were conducted for two cases of non-corroded and corroded model simulating test specimen. Figure 10 shows assumed plate thickness of corroded model which reflects the measured data. Average thickness reductions were 2.0mm for the diagonal flange, 3.0mm for the diagonal web and 4.0mm for the gusset plate, respectively.

Experimental and Analysis Results

Figure 11 shows the curves of load versus vertical displacement at the loading head. The analytical ultimate strengths were 4953kN for the un-corroded model and 3346kN for the corroded model. The ratio of the strengths is about 2/3, which is similar to average thickness loss of the gusset plate. The measured ultimate strength was 3598kN, that is about 1.1 times the analytical value for the corroded model. Linear behavior was observed until the out-of-plane deformation of gusset plate become large. After that, the load reached maximum load gradually and fell down moderately. The measured value and analytical value show generally the same curves and ultimate loads.

Figure 12 shows failed specimen after the test. The failure mode of the specimens was plate local buckling of the gusset. Figure 13 shows out-of-plane deformation and relations between load and the deformation of the both side of gusset plates at major points. With increase of vertical load, deformation of one side of the gusset plate preceded with the other side of the gusset. As a result, the buckling shape of unsupported edge shows unsymmetry. As for the analytical results of the corroded model, Von Mises stress contours and yielded area at the peak load are shown in Figure 14 and Figure 15, respectively. The local buckling occurred at the plate area underneath the diagonals and free edges of the gusset plate. Figure 16 compares the out-of-plane deformation at major points where large deformations were measured and shows good agreement. For reference, analytical out-of-plane deformation contours of the corroded model are also shown in this figure. The results in these figures provide verification of the corroded model using shell element to evaluate compressive behavior of the corroded gusset plate connection. About the modeling of the corrosion, the use of average reduction thickness of gusset plate seems reasonable to evaluate the behavior of the gusset plate in this specimen, however detailed investigation is required. Figure 17 shows the out-of-plane displacement along the line parallel to the centerline of the compression diagonal.

Strength Estimation Equations of Truss Gusset Plate Connections

Strength Equations

After the collapse of I-35W Bridge, “Load Rating Guidance and Examples for Bolted and Riveted Gusset Plates in Truss Bridges” [2] was issued by FHWA in 2009. By referencing the Guidance and previous experimental research results [3]- [7], limit state of gusset plate and diagonal members are assumed as follows as shown in Figure 18,

a) Strength of fasteners in compression and tension
b) Cross section yielding or net section fracture strength of gusset plate
c) Block shear rupture strength in tension
d) Cross section yielding or net section fracture strength of diagonal member
e) Compressive strength
f) Shear fracture strength

This paper only discusses compressive strengths of b), d) and e). The resistance factors are1.0 in this study.

Cross section yielding strength of gusset plate in compression

The Whitmore effective width[3] is used for estimating yielding of the gusset plate. The effective width is bound on either side by the closer of the nearest adjacent plate edges or lines constructed starting from the external fasteners within the first row and extending from these fasteners at an angle of 30 degrees with respect to the line of action of the axial force (see Figure 19). The cross section yielding is taken as:

$$P_{gy} = f_y A_e \tag{1}$$

where:

A_e:gross cross-sectional area of Whitmore effective width of the plate, A_e=$L_e t$(mm^2)
f_y: yield strength of the plate (N/mm^2)
L_e:Whitmore effective width (see Figure 19)(mm)
t: thickness of the plate (mm)

Cross section yielding of diagonal member

The smallest sectional area of the diagonal members near the gusset plate boundary is assumed to be yielded. The cross section yielding strength is expressed by:

$$P_{dy} = f_y A_g \tag{2}$$

where:

f_y: yield strength of the diagonal (N/mm^2)
A_g: gross cross-sectional area of the diagonal (mm^2)

Local buckling at the plate area underneath the splice member of diagonals

The Whitmore effective width and an unbraced gusset plate length which is average of the three lengths was used for estimating buckling strength. Standard buckling equations specified in Japanese Design code (JSHB) was used. Ignoring any lateral constraint to the gusset plate, the effective length factor, β (β=1.2) was used for unbraced gusset plate assuming the buckled shape as shown in Figure 20. The local buckling equation is taken as:

$$P_{gcr} = f_y A_g \qquad (\bar{\lambda} \leqq 0.2) \tag{3a}$$

$$P_{gcr} = (1.109 - 0.545\bar{\lambda}) f_y A_g \qquad (0.2 < \bar{\lambda} \leqq 1.0) \tag{3b}$$

$$P_{gcr} = (1.0/(0.773 + \bar{\lambda}^2) f_y A_g \qquad (1.0 < \bar{\lambda}) \tag{3c}$$

where:

f_y: yield strength of the plates (N/mm^2)
A_g: gross cross-sectional area (mm^2)

The column slenderness ratio $\bar{\lambda}$ is given by:

$$\bar{\lambda} = \frac{1}{\pi} \cdot \sqrt{\frac{f_y}{E}} \cdot \frac{\beta L_c}{r_s} \qquad (4)$$

where:

E: Young's modulus of plate (N/mm^2)

β: effective length factor (=1.2)

L_c: $L_c = (L_1+L_2+L_3)/3$

L_1, L_2, L_3: distance from center or each end of the Whitmore width to the edge in the closest adjacent member, measured parallel to the line of action of the compressive axial force (see Figure 19).

r_s: radius of gyration about the plane of buckling, $r_s = \sqrt{I_g / A_g}$ (mm)

I_g : moment of inertia (mm^4)

Comparison of Analysis Results and Calculation Results

Table 2 outlines the comparison of the experimental results, FE analysis results and the calculation results for the specimen. The ratio means the calculated or measured value to the analytical value. The calculated yield strength by the Whitmore effective width was to some extent close to the analytical ultimate strength with ratios of 0.97 (un-corroded model) and 0.95 (corroded model). On the other hand, the calculated yield strength of the diagonal was larger than the analytical value with ratios of 1.23 and 1.39. It is indicated that the gusset plate failure preceded with yielding of the diagonal. Strength equation for local buckling gives conservative estimates with strength ratio of 0.59 (un-corroded model) and 0.36 (corroded model), much below 1.0.

Regarding the compressive strength of the gusset plate connection, the results in this study were compared with experimental results[4]-[8]. Figure 21 shows comparison of the measured ultimate loads and the calculated values for local buckling and yielding respectively. Figure 22 shows relations of ultimate strength and slenderness ratio. Calculated values are also conservative for the experimental data, and the correlation is not good. Then, we are investigating more accurate estimation of ultimate strength of the gusset plate. According to the failure mode, the ultimate strength is likely to depend on the buckling strength of the compressive unbraced area parts and the strength of its surrounding plate area. As one of our ideas, we are trying to evaluate the compressive strength by the summation of following strength equations of gusset plate divided into 3 areas as shown in Figure 23.

$$P_{gcr} = P_{gcr1} + P_{gcr2} + P_{gsy} \qquad (5)$$

P_{gcr1} is expressed by:

$$P_{gcr1} = f_y A_g \qquad (\bar{\lambda} \leqq 1.0) \tag{6a}$$

$$P_{gcr1} = \frac{1}{\bar{\lambda}^2} f_y A_g \qquad (1.0 < \bar{\lambda}) \tag{6b}$$

The column slenderness ratio $\bar{\lambda}$ is given by:

$$\bar{\lambda} = \frac{1}{\pi} \bullet \sqrt{\frac{f_y}{E}} \bullet \frac{\beta L_c}{r_s} \tag{7}$$

where:

β: effective length factor (=0.65)

L_c: $L_c = (L_1+L_2+L_3) / 3$

L_1, L_2, L_3: The distance from center or each end of the width of diagonal end to the edge in the closest adjacent member, measured parallel to the line of action of the compressive axial force (see Figure 23).

P_{gcr2} is expressed by:

$$P_{gcr2} = f_y A_g \sin\theta_1 \qquad (R \leqq 1.0) \tag{8a}$$

$$P_{gcr2} = \frac{1}{R^2} f_y A_g \sin\theta_1 \qquad (1.0 < R) \tag{8b}$$

The plate slenderness ratio R is given by:

$$R = \frac{b}{t} \bullet \sqrt{\frac{f_y}{E} \bullet \frac{12(1-\nu^2)}{\pi^2 k}} \tag{9}$$

where:

ν: The Poisson's ratio (=0.3)

k: The buckling coefficient , $k = \frac{4}{\alpha^2} + \frac{40}{3\pi^2} + \frac{15\alpha^2}{\pi^4} - \frac{20\nu}{\pi^2}$

α: $\alpha = h_c \ / \ b_2$

h_c: $h_c = (h_1+h_2) / 2$

P_{gsy} is expressed by:

$$P_{gsy} = \frac{f_y}{\sqrt{3}} A_g \cos\theta_2 \tag{10}$$

Figure 24 shows comparison of the measured ultimate loads and the calculated values. It is noticed that failure modes of all data are local buckling, not compressive and block shear failure which is described in [8]. Considering that previous experimental data contain various gusset configurations, it appears the ultimate strength can be approximately estimated. Still there is a difference, further study is required to estimate the ultimate strength for compressive load.

Conclusions

Compressive loading test of the corroded gusset plate connection specimen from decommissioned truss bridge was performed, and the FE analyses were conducted to complement experimental results. As for compressive strength estimation of gusset plate connection, from practical viewpoint, application of strength equations were discussed with use of previous experimental research results. The major findings are summarized as follows.

1) Based on thickness loss measurement of gusset plate connection, advanced corrosion of diagonals and gusset plate was observed around the connection parts. Severe corrosion part generally corresponded to the part where large stresses appear.

2) The effect of the section loss on the compressive strength of the gusset plate was evaluated by experimental and analytical results. Compressive behavior of the gusset plate was properly evaluated by shell element model in consideration of the average thickness reduction.

3) Local buckling strengths by the Whitmore effective width provided conservative estimates to the experimental ultimate strength. Taking the buckling strength of the compressive area and the strength of its surrounding plate area into consideration gave more proper prediction.

Acknowledgment

This research was undertaken as part of the collaborative research project between Public Works Research Institute; Tokyo Metropolitan University; and Waseda University, and funded by the Ministry of Land, Infrastructure, Transport and Tourism based on the Construction Technology Research and Development Subsidy Program. Finally, the authors express appreciation to Choshi Public Works Office, Chiba Prefecture for their cooperation.

References

[1] Japan Road Association (JRA), "Specification for Highway Bridges, Part II Steel Bridge", 2002.(in Japanese)
[2] Federal Highway Administration, "Load Rating Guidance and Examples For Bolted and Riveted Gusset Plates In Truss Bridges", Publication No.FHWA-IF-09-014, 2009.
[3] Whitmore, R.E., "Experimental Investigation of Stresses in Gusset Plates, Bulletin No.16, Engineering Experiment Station", University of Tennessee,1952.
[4] Yam, M. and Cheng, J., "Experimental Investigation of the Compressive Behavior of Gusset Plate Connections", Structural Engineering Report No.194, Dept. of Civil Engineering, University of Alberta,1993.

[5] Ocel, J. M., Hartman, J.L., Zobel, R.,White, D. and Leon, R., " Inspection and Rating of Gusset Plates - A Response to the I-35W Bridge Collapse", Proceedings of the 26th US-Japan Bridge Engineering Workshop, pp.11-23, 2010.
[6] Matsuhisa, S., Yamamoto, K. and Okumura, T., "Loading Experiment of Truss Gusset Plate Connections", Proceedings of the 31st Annual Conference of Japan Society of Civil Engineers, pp.297-298, 1976. (in Japanese)
[7] Matsuhisa, S., Yamamoto, K. and Okumura, T., "Loading Experiment of Truss Gusset Plate Connections", Proceedings of the 32nd Annual Conference of Japan Society of Civil Engineers, pp.631-632, 1978.(in Japanese)
[8] Kasano, H., Yoda, T., Nogami, K., Murakoshi, J., Toyama, N., Sawada, M., Arimura, K. and Guo, L., "Study on Failure modes of Steel Truss Bridge Gusset Plates Related to Compression and Shear Block Failure", Proceedings of the 66th Annual Conference of Japan Society of Civil Engineers, pp.149-150, 2011. (in Japanese)

Figure 1 Old Bridge and New Bridge (cable-stayed bridge)

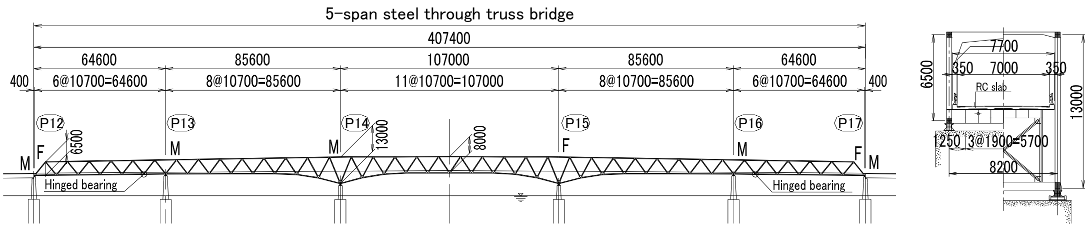

Figure 2 General View of Choshi Bridge

a) Lower chord connection

b) Upper chord connection

c) Plate bonding of lower chord connection

d) Diagonal joint

e) Pitting of diagonal

f) Section loss of end floor beam

Figure 3 Corrosion Damage of Main Members

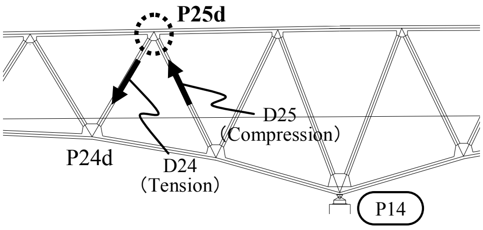

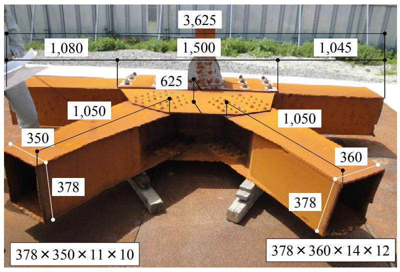

a)The test Specimen

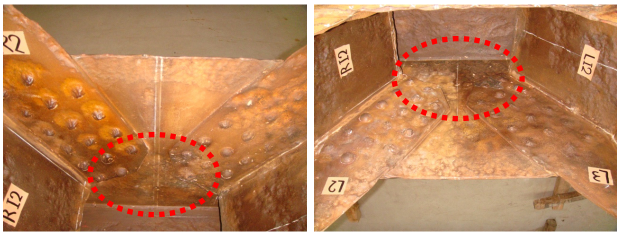

b) The edge of flange

c) Inside gusset plate connection

Figure 4　P25d Connection Cut Out as Specimen

Table 1　Design Axial Force and Design Stress

Design load	D24(Compression)		D25(Tension)		Notes
	Axial force(kN)	Stress(MPa)	Axial force (kN)	Stress(MPa)	
Dead load	1,027	69	-973	-52	
Live load	785	53	-742	-40	TL-20
Total (Ratio)	1,812(-1.06)	112	-1,715(1.0)	-92	
Allowable stress	—	128	—	-93	SM40

Figure 5 Thickness Loss Measurement by Laser Measurement Epuipment

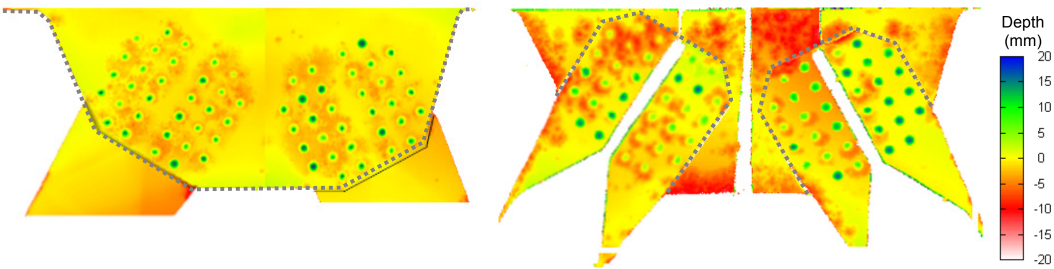

a) Outside gusset plate

b) Inside gusset plate

Figure 6 Thickness Reduction of Corroded Specimen

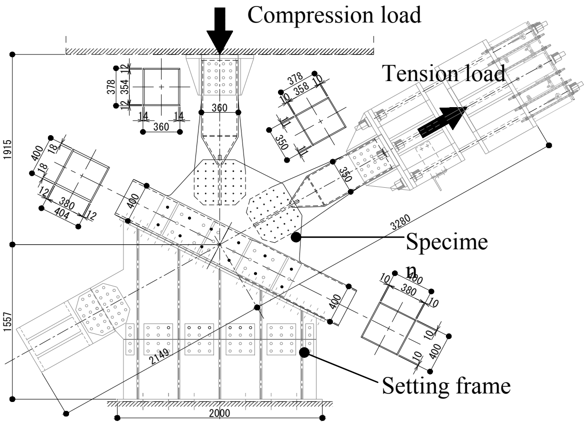

Figure 7 Outline of Specimen and Loading Frame

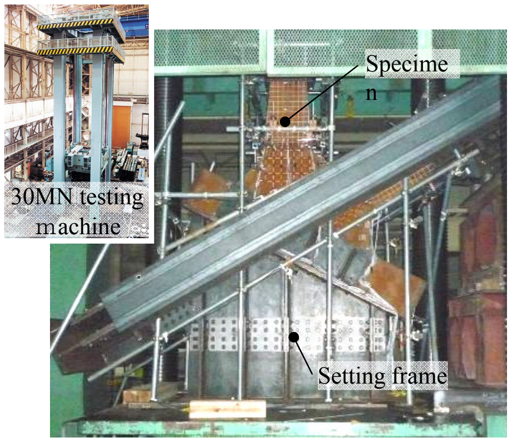

Figure 8 Test Setup of P25d Connection

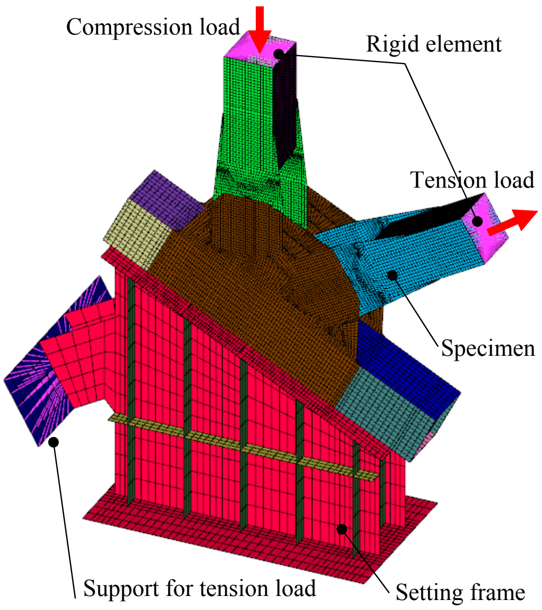

Figure 9   Analysis Model

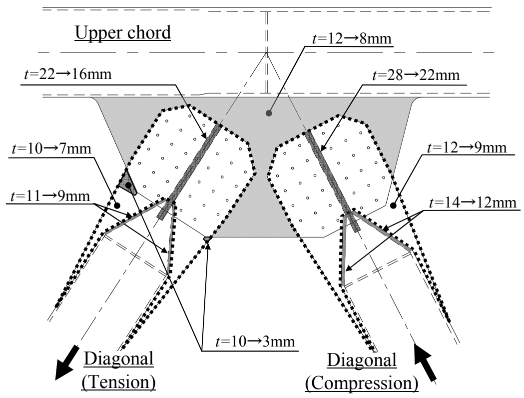

Figure 10 Plate Thickness Reduction of Corroded Model

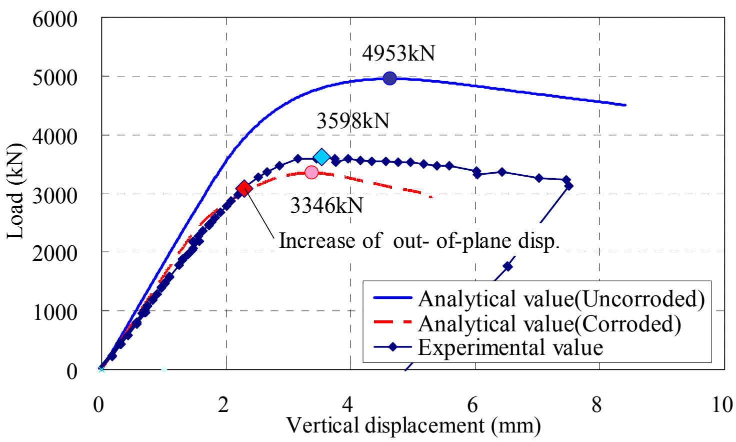

Figure 11 Compression Load vs. Vertical Displacement Curves

Figure 12 Failed Specimen after the Test

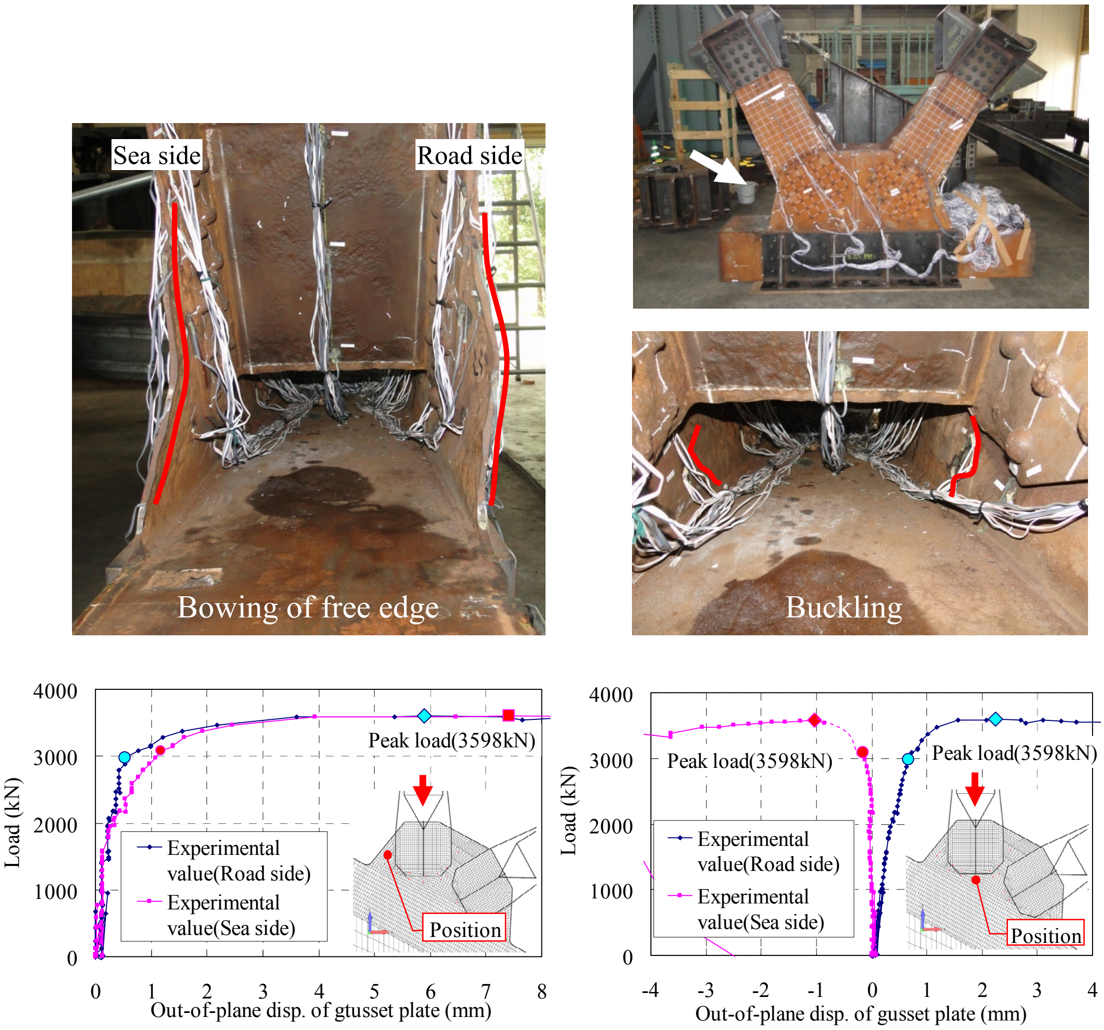

a) Free edge of gusset   b) Unbraced area of gusset

Figure 13 Compression Load vs. Out-of-displacement of gusset plate Curves

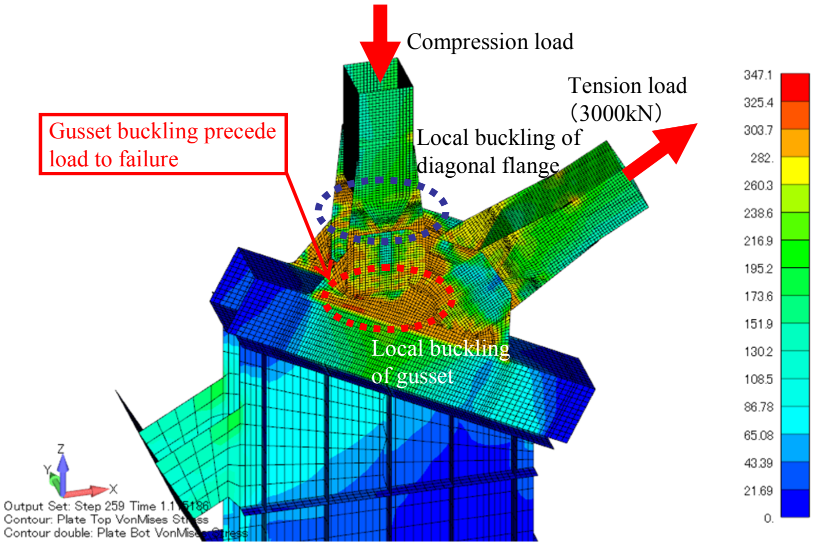

Figure 14 Von Mises Stress Contour of Corroded Model Gusset at Peak Load

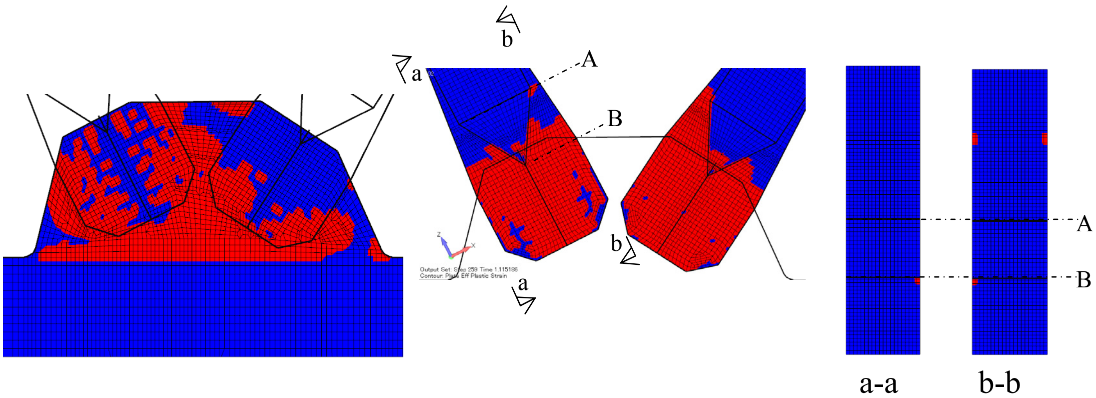

a) Outside surface of gusset b) Outside surface of diagonal

Figure 15 Yield Strain Distribution of Outside Web at Peak Load

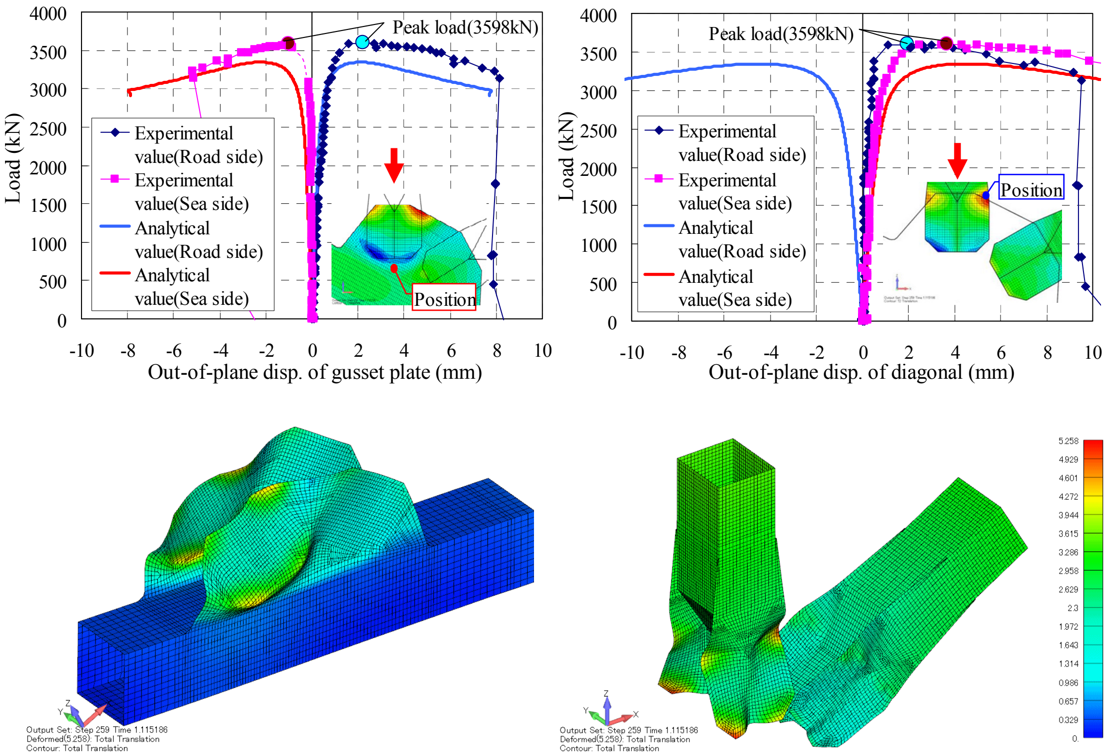

a) Unbraced area of gusset b) Free edge of diagonal

Figure 16 Load vs. Out-of-plane Displacement Curves

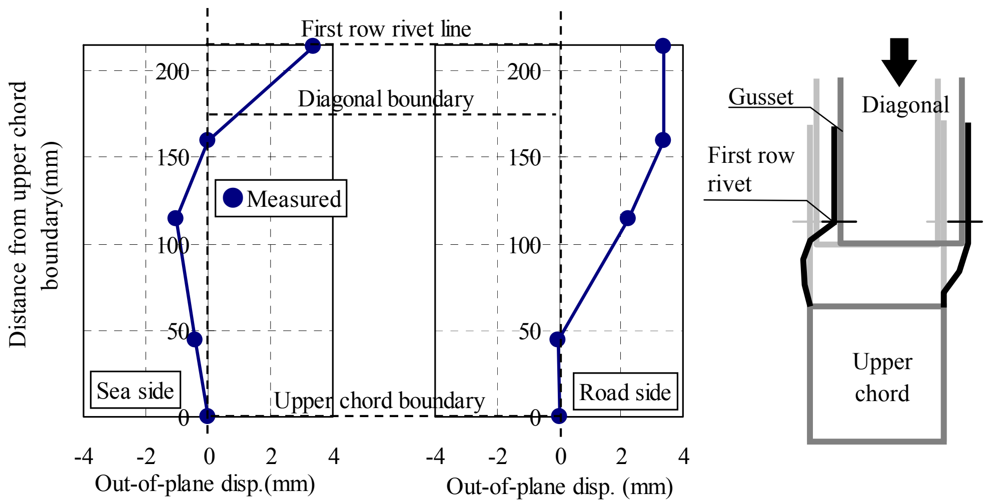

Figure 17 Deflected Mode of Unbraced Area

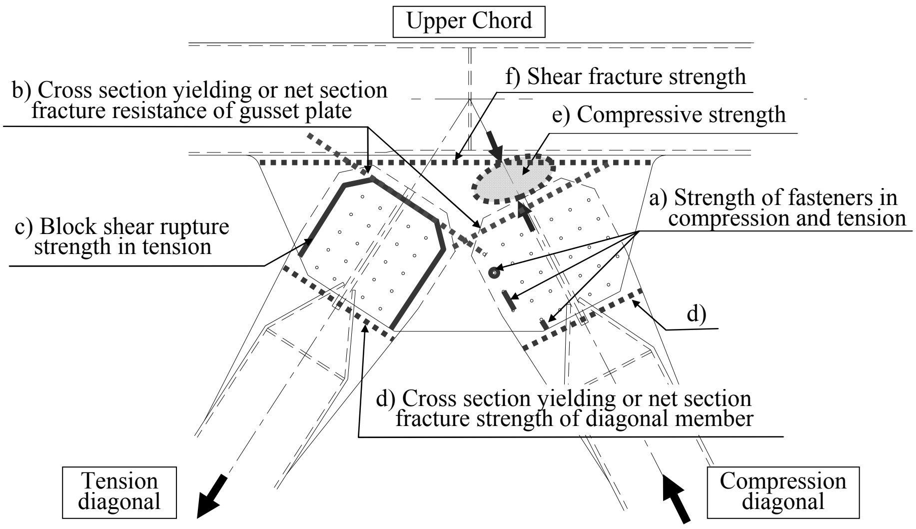

Figure 18 Limit State of Gusset Plate Connection

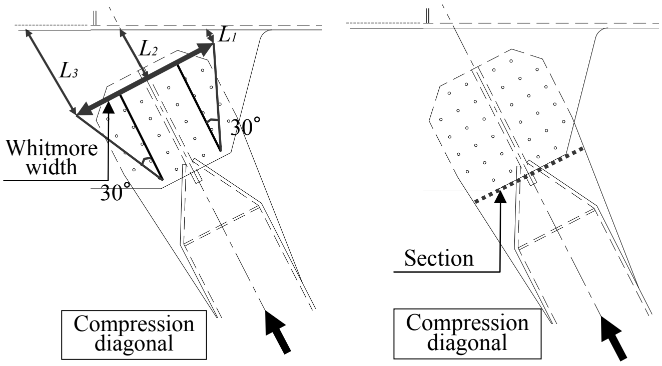

a)Yielding or local buckling of gusset plate

b) Yielding of diagonal

Figure 19 Strength Equations for Compression

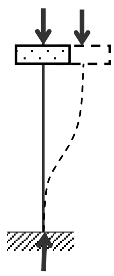

Figure 20 Effective length Factor (β=1.2)

Table 2 The Comparison of the Ultimate Strength

Compressive ultimate strength			Uncorroded model	Corroded model
Analysis Value (Ultimate Load)		kN (ratio)	4,953 (1.00)	3,346 (1.00)
Calculated Value	b) Cross section yielding of gusset plate	kN (ratio)	4,792 (0.97)	3,194 (0.95)
	d) Cross section yielding of diagonal member	kN (ratio)	6,087 (1.23)	4,666 (1.39)
	e) Compressive strength	kN (ratio)	2,948 (0.59)	1,220 (0.36)
Experimental Value (Ultimate Load)		kN (ratio)	—	3,598 (1.08)

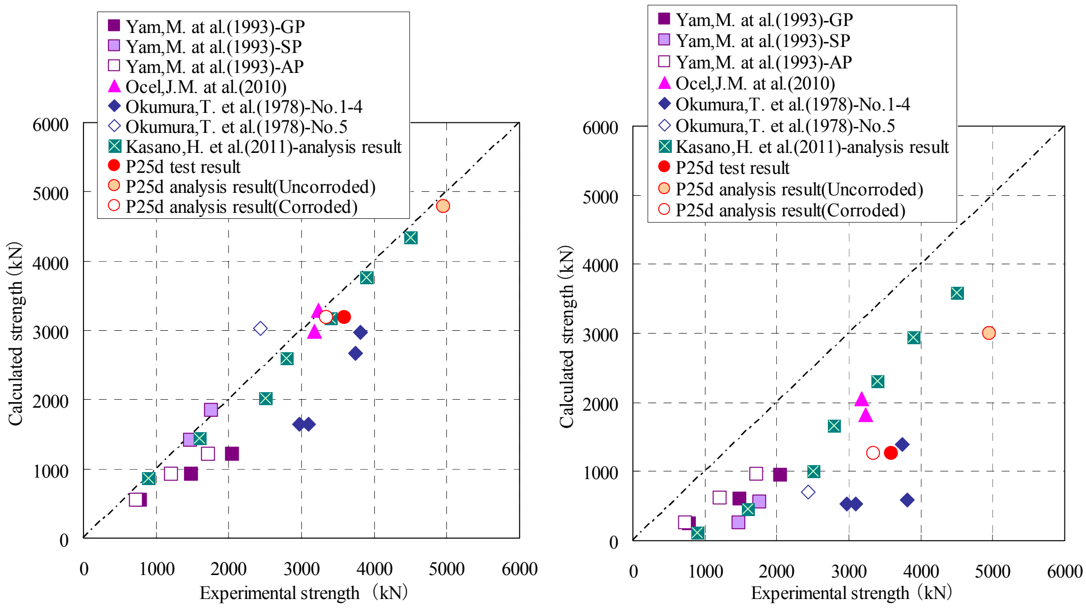

a) Yielding　　　　　　　　b) Local buckling

Figure 21 Comparison of the Experimental Ultimate Strength and the Calculated Strength

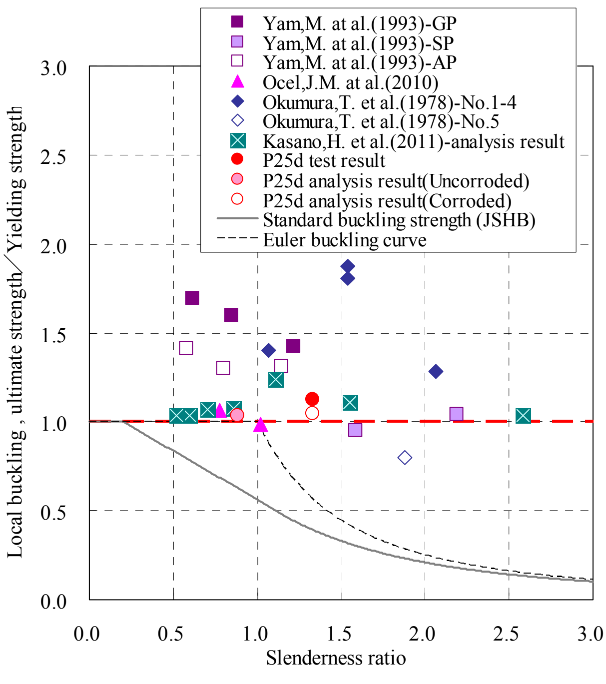

Figure 22 Relations of Strength and Slenderness Ratio

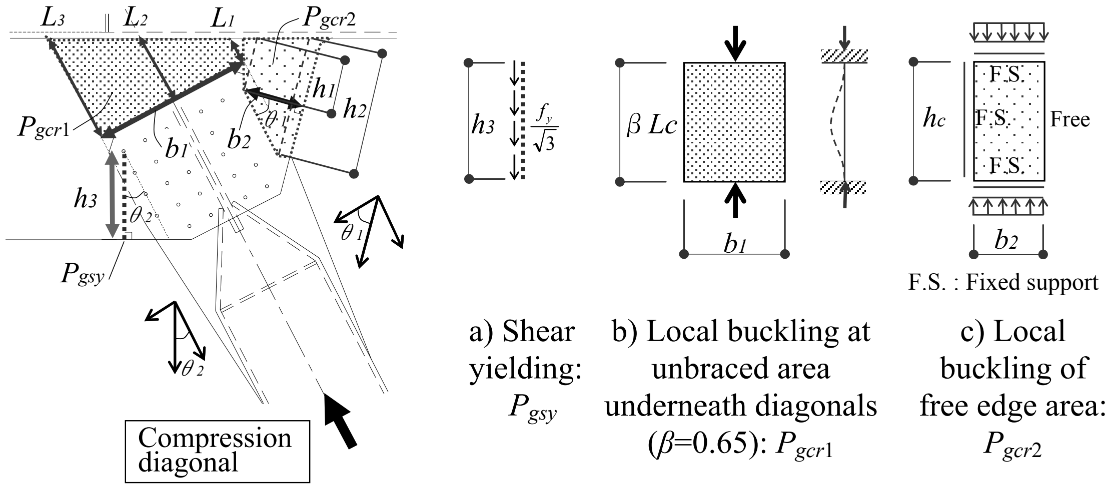

Note : θ_1 is angle between diagonal axis and line b_2.
θ_2 is angle between diagonal axis and line h_3.

Figure 23 Model for Estimating Compression Ultimate Strength of Gusset Plate

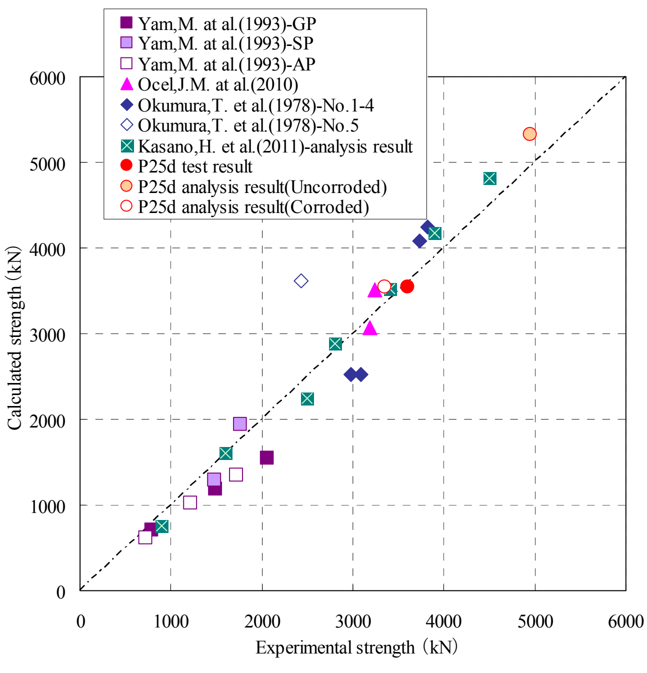

Figure 24 Comparison of the Experimental Strength and the Calculated Strength